THE JOURNAL OF BIOLOGICAL CHEMISTRY VOL. 286, NO. 25, pp. 22570–22579, June 24, 2011

Crystal Structure of the Ca^{2+}/Calmodulin-dependent Protein Kinase Kinase in Complex with the Inhibitor STO-609*[S]

Received for publication, April 15, 2011 Published, JBC Papers in Press, April 19, 2011, DOI 10.1074/jbc.M111.251710

Mutsuko Kukimoto-Niino[‡], Seiko Yoshikawa[‡], Tetsuo Takagi[‡], Noboru Ohsawa[‡], Yuri Tomabechi[‡], Takaho Terada[‡], Mikako Shirouzu[‡], Atsushi Suzuki[§], Suni Lee[§], Toshimasa Yamauchi[¶], Miki Okada-Iwabu[¶], Masato Iwabu[¶], Takashi Kadowaki[¶], Yasuhiko Minokoshi[§1], and Shigeyuki Yokoyama[‡‖2]

From the [‡]RIKEN Systems and Structural Biology Center, Yokohama 230-0045, the [§]National Institute for Physiological Sciences, Aichi 444-8585, and the [¶]Graduate School of Medicine and [‖]Graduate School of Science, The University of Tokyo, Tokyo 113-0033, Japan

Ca^{2+}/calmodulin (CaM)-dependent protein kinase (CaMK) kinase (CaMKK) is a member of the CaMK cascade that mediates the response to intracellular Ca^{2+} elevation. CaMKK phosphorylates and activates CaMKI and CaMKIV, which directly activate transcription factors. In this study, we determined the 2.4 Å crystal structure of the catalytic kinase domain of the human CaMKKβ isoform complexed with its selective inhibitor, STO-609. The structure revealed that CaMKKβ lacks the αD helix and that the equivalent region displays a hydrophobic molecular surface, which may reflect its unique substrate recognition and autoinhibition. Although CaMKKβ lacks the activation loop phosphorylation site, the activation loop is folded in an active-state conformation, which is stabilized by a number of interactions between amino acid residues conserved among the CaMKK isoforms. An *in vitro* analysis of the kinase activity confirmed the intrinsic activity of the CaMKKβ kinase domain. Structure and sequence analyses of the STO-609-binding site revealed amino acid replacements that may affect the inhibitor binding. Indeed, mutagenesis demonstrated that the CaMKKβ residue Pro^{274}, which replaces the conserved acidic residue of other protein kinases, is an important determinant for the selective inhibition by STO-609. Therefore, the present structure provides a molecular basis for clarifying the known biochemical properties of CaMKKβ and for designing novel inhibitors targeting CaMKKβ and the related protein kinases.

Calcium is a ubiquitous second messenger that modulates diverse cellular responses. The Ca^{2+} receptor protein calmodulin (CaM)[3] is involved in Ca^{2+} signaling through its effects on a variety of CaM-binding proteins, including a family of Ser/Thr protein kinases known as Ca^{2+}/CaM-dependent protein kinases (CaMKs). The members of this family, CaMKI, CaMKIV, and CaMK kinase (CaMKK), constitute the CaMK cascade that directly activates transcription factors, such as cAMP-response element-binding protein, thereby regulating Ca^{2+}-dependent gene expression (1–4). CaMKK phosphorylates the equivalent Thr residues of CaMKI and CaMKIV (Thr^{177} and Thr^{196}, respectively) and enhances their activities (5, 6). There are two mammalian CaMKK isoforms, CaMKKα and CaMKKβ, which are localized in the cytoplasm and the nucleus, respectively (7–9). Extensive cross-talk between the CaMK cascade and other signaling pathways has been demonstrated. For example, the CaMK cascade activates the MAP kinases, such as the extracellular signal-regulated kinase (ERK) and the c-Jun N-terminal kinase (JNK) (10, 11). The CaMKK activity can be suppressed through phosphorylation by the cAMP-dependent kinase (PKA) (12). CaMKK directly phosphorylates and activates protein kinase B (PKB) and modulates apoptosis (13). CaMKK also activates the AMP-activated protein kinase (AMPK), a critical regulator of energy balance (14). Recently, a brain-specific AMPK family member, SAD-B, has been identified as a novel CaMKK target (15).

The members of the CaMK cascade share a common domain organization: the catalytic kinase domain (KD) and the C-terminal autoinhibitory domain (AID), which partially overlaps with the CaM-binding domain (CBD) (16) (see Fig. 1*A*). The crystal structure of the CaMKI KD-AID fragment revealed that the interaction of KD with AID prevents both substrate and ATP binding and maintains the kinase in an inactive state (17). Ca^{2+}/CaM binding relieves the autoinhibition of the kinase, although the CaM·CBD complex structures determined previously for CaMKK and CaMKI revealed different interaction modes (18–20).

Previous studies demonstrated the different biochemical properties between the CaMKK isoforms (21–23); the CaMKKα activity is strictly regulated by Ca^{2+}/CaM, whereas CaMKKβ exhibits significant "autonomous" activity (60–70% of the total activity) in the absence of Ca^{2+}/CaM. A 23-amino

* This work was supported by grants from the RIKEN Structural Genomics/Proteomics Initiative (RSGI), the National Project on Protein Structural and Functional Analyses, and the Targeted Proteins Research Program (TPRP), the Ministry of Education, Culture, Sports, Science and Technology of Japan.

The atomic coordinates and structure factors (code 2ZV2) have been deposited in the Protein Data Bank, Research Collaboratory for Structural Bioinformatics, Rutgers University, New Brunswick, NJ (http://www.rcsb.org/).

[S] The on-line version of this article (available at http://www.jbc.org) contains supplemental Fig. 1.

[1] To whom correspondence may be addressed: Division of Endocrinology and Metabolism, Department of Developmental Physiology, National Institute for Physiological Sciences, Okazaki, Aichi 444-8585, Japan. Tel.: 81-564-55-7745; Fax: 81-564-55-7741; E-mail: minokosh@nips.ac.jp.

[2] To whom correspondence may be addressed: Shigeyuki Yokoyama, RIKEN Systems and Structural Biology Center, 1-7-22 Suehiro-cho, Tsurumi-ku, Yokohama 230-0045, Japan. Tel.: 81-45-503-9196; Fax: 81-45-503-9195; E-mail: yokoyama@biochem.s.u-tokyo.ac.jp.

[3] The abbreviations used are: CaM, calmodulin; CaMK, CaM-dependent protein kinase; CaMKK, CaMK kinase; AMPK, AMP-activated protein kinase; KD, kinase domain; AID, autoinhibitory domain; CBD, CaM-binding domain; RP-insert, Arg-Pro-rich insert.

acid region (residues 129–151) at the N terminus of rat CaMKKβ was identified as the regulatory domain that relieves the kinase from autoinhibition, thus allowing its Ca^{2+}/CaM-independent activity (23).

Ser^{74}, Thr^{108}, and Thr^{458} of rat CaMKKα are the inhibitory sites phosphorylated by PKA. Phosphorylation of Thr^{458} within the CBD suppresses the CaM binding to CaMKK (12). Phosphorylation of Ser^{74} in the region N-terminal to the KD promotes the binding of protein 14-3-3, which suppresses the CaMKK activity (24). Intriguingly, the three PKA-mediated phosphorylation sites are conserved throughout the isoforms and species, suggesting the existence of a common mechanism of intramolecular regulation among the CaMKKs.

We now report the crystal structure of the human CaMKKβ KD complexed with STO-609, a selective inhibitor of CaMKK. STO-609 inhibits both the CaMKKα and the CaMKKβ isoforms, but CaMKKβ is more sensitive to STO-609 than CaMKKα (25). The CaMKKβ·STO-609 complex structure determined in this study provides a basis for understanding the selective inhibition of CaMKKβ by STO-609 as compared with CaMKKα and other protein kinases. We also report the first evidence that CaMKKβ lacks the activation loop phosphorylation site, which accounts for its high autonomous activity, and discuss the other structural properties of CaMKKβ that reflect its unique substrate recognition and autoinhibition.

TABLE 1
Crystallographic statistics
All numbers in parentheses refer to the highest resolution shell statistics.

Data collection	
Wavelength (Å)	1.00
Space group	$P2_12_12_1$
Cell dimensions	
a, *b*, *c* (Å)	69.4, 77.2, 84.3
α, β, γ (°)	90, 90, 90
Resolution range (Å)	50–2.4 (2.49–2.40)
Redundancy	4.5
Unique reflections	17,475
Completeness (%)	98.5 (99.9)
$I/\sigma(I)$	25.9 (2.8)
R_{sym}[a]	0.057 (0.607)
Refinement	
Resolution range (Å)	37.0–2.40 (2.55–2.40)
No. of reflections	16,795
R-factor/Free *R*-factor[b]	0.203/0.252
No. of atoms	
Protein	2066
Ligand	24
Water	53
Average *B*-values (Å^2)	
Protein	50.1
Ligand	35.7
Water	40.4
r.m.s.[c] deviations	
Bond lengths (Å)	0.006
Bond angles (°)	1.3
Ramachandran plot	89.3, 9.4, 0.9, 0.4

[a] $R_{sym} = \sum |I_{avg} - Ii| / \sum Ii$, where *Ii* is the observed intensity and I_{avg} is the average intensity.
[b] Free *R*-factor is calculated for 5% of randomly selected reflections excluded from refinement.
[c] r.m.s., root mean square.

EXPERIMENTAL PROCEDURES

Plasmids—The human CaMKKβ cDNA clone was obtained from the Kazusa collection (Kazusa clone ID: KIAA0787). Throughout this study, we utilize the residue numbers of Fig. 1*B*, according to the human CaMKKβ protein (Swiss-Prot accession code: Q96RR4) with the N terminus at Met^1. The DNA encoding human CaMKKβ KD (residues 158–448) was subcloned into the expression vector pCR2.1 TOPO (Invitrogen) as a fusion with an N-terminal His tag and a tobacco etch virus protease cleavage site. The expression plasmid for the human CaMKI KD (residues 1–281) (OriGene Technologies) for use in kinase assays was similarly constructed. Point mutations were introduced into the CaMKKβ and CaMKI KDs by using a QuikChange site-directed mutagenesis kit (Stratagene).

Protein Expression and Purification—The protein was synthesized by the *Escherichia coli* cell-free system (26, 27). The internal solution was dialyzed in dialysis tubes (Spectra/Por 7 molecular weight cut-off, 15,000; Spectrum) against the external solution at 30 °C for 2.5 h with shaking, and then it was centrifuged at 16,000 × *g* at 4 °C for 20 min. The supernatant was loaded onto a HisTrap (GE Healthcare) column and eluted with a buffer containing 20 mM Tris-HCl (pH 8.0), 500 mM NaCl, 10% glycerol, and 500 mM imidazole. The eluate was incubated overnight with tobacco etch virus protease to cleave the His tag and was dialyzed against 20 mM Tris-HCl (pH 8.0), 150 mM NaCl, 10% glycerol, and 20 mM imidazole. To separate the His tag and the tobacco etch virus protease, the protein was loaded on a HisTrap column, and the flow-through fractions were collected. The protein was further purified by ion exchange on a HiTrap Q column and size-exclusion chromatography on a Superdex 200 column (GE Healthcare), in a final buffer containing 20 mM Tris-HCl (pH 7.5), 300 mM NaCl, 10% glycerol, and 2 mM DTT.

Crystallization and Data Collection—Before crystallization, the purified protein (8.0 mg/ml) was mixed with 1 mM STO-609 (Sigma-Aldrich) and 5 mM $MgCl_2$ and was incubated at 4 °C overnight. Diffraction quality crystals of CaMKKβ complexed with STO-609 were grown in drops composed of 1 μl of protein solution, 1 μl of 0.5% agarose solution (Hampton Research), and 1 μl of reservoir solution, containing 0.1 M sodium cacodylate (pH 5.9), 0.2 M sodium acetate, and 18% PEG8000 (Hampton Research), by the hanging drop vapor diffusion method at 20 °C. Data collection was performed at 100 K, with the reservoir solution containing 29% glycerol as a cryoprotectant. The data were collected at a wavelength of 1.0 Å at BL41XU, SPring-8 (Hyogo, Japan) and were recorded on an MX225-HE CCD detector. The diffraction data were processed with the HKL2000 program (28).

Structure Determination and Refinement—The structure was solved by the molecular replacement method with the program PHASER (29, 30), using the structure of human CaMKIIδ isoform 1 (Protein Data Bank (PDB) code 2VN9) as the search model. The model was corrected iteratively using the program Coot (31), and the structure refinement was performed with the Crystallography and NMR System (CNS) (32). All refinement statistics are presented in Table 1. The quality of the model was inspected by the program PROCHECK (33). Structural similarities were calculated with the program Dali (34). The graphic figures were created using the program PyMOL (35).

Kinase Assays—The AMPK peptide, including the sequence surrounding the phosphorylation site of AMPK

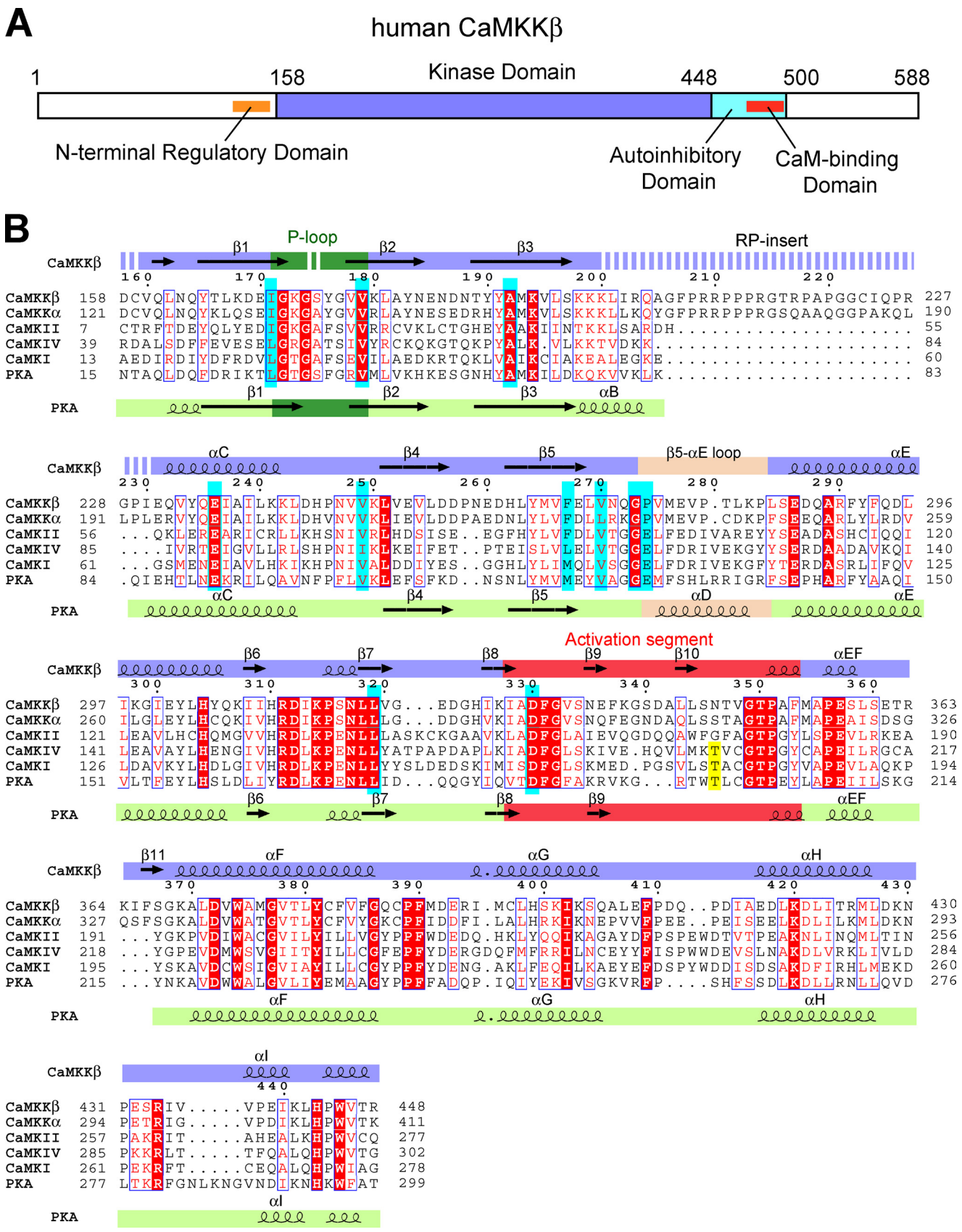

FIGURE 1. **Primary structure of CaMKKβ.** *A*, domain organization of human CaMKKβ. *B*, sequence alignment of the KDs of human CaMKKβ, human CaMKKα, human CaMKI, human CaMKIV, and mouse PKA. The STO-609-interacting residues are colored *cyan*, and the activation loop phosphorylation sites are *yellow*. The secondary structural elements of CaMKKβ and PKA are indicated above and below the sequences, respectively. The glycine-rich P-loop is colored *green*, the activation segment is *red*, and the β5-αE loop (CaMKKβ) and the helix αD (PKA) are *wheat*. Disordered regions are indicated as *dashed lines*. This figure was generated using the program ESPript (49).

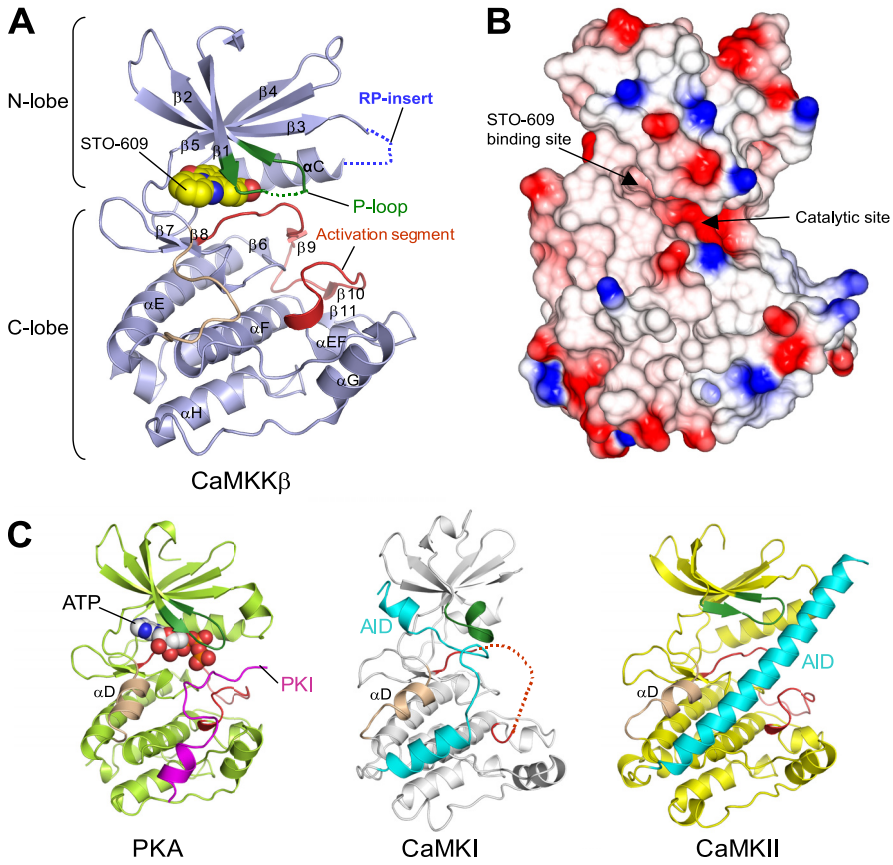

FIGURE 2. **Structure of the CaMKKβ·STO-609 complex.** *A*, ribbon representation of the CaMKKβ KD structure. The P-loop is colored *green*, the activation segment is *red*, and the β5-αE loop is *wheat*. The STO-609 is shown in a *sphere representation*. Disordered regions are indicated as *dashed lines*. *B*, the electrostatic surface of the CaMKKβ KD (*red*, negative charge; *blue*, positive charge), shown in the same orientation as in *A*. The locations of the STO-609-binding site and the catalytic site are indicated. This figure was generated using the program CCP4 MG (50). *C*, structure comparison with other protein kinases. Structures of the PKA KD complexed with PKA inhibitor (*PKI*) (*left*), the CaMKI KD-AID (*middle*), and the CaMKII KD-AID (*right*), shown in the same orientation as that of CaMKKβ (*A*). In these KD structures, the P-loop is colored *green*, the activation segment is *red*, and the helix αD is *wheat*. The PKI bound to PKA is colored *magenta*, and the AIDs of CaMKI and CaMKII are *cyan*. The ATP bound to PKA is shown in a *sphere representation*.

(^{167}GEFLRTSCGSP^{177}), was synthesized at the Support Unit for Bio-material Analysis in the RIKEN Brain Science Institute (BSI) Research Resources Center (RRC). Appropriate quantities of the purified CaMKKβ KD and full-length CaMKKβ (Carna Biosciences) were each incubated in the presence or absence of 500 μM AMPK peptide at 30 °C, in a reaction solution (20 μl) containing 50 mM HEPES (pH 7.5), 300 mM NaCl, 1 mM DTT, 10 mM $MgCl_2$, 400 μM ATP, and 10% glycerol, with or without 0.5 μM STO-609. For the full-length CaMKKβ, 5 μM calmodulin (Sigma-Aldrich) and 1 mM $CaCl_2$ were added to the reaction solution. ATP consumption was determined by using a Kinase-Glo™ Max luminescent kinase assay (Promega) kit, which quantifies the amount of ATP in the reaction solution. Glow-type luminescence was recorded after 10 min, using a Fusion™ universal microplate analyzer (Packard).

RESULTS AND DISCUSSION

Overall Structure—We crystallized human CaMKKβ KD (residues 158–448) in the presence of STO-609. The crystal belongs to the primitive orthorhombic space group $P2_12_12_1$ with unit cell constants of $a = 69.4$ Å, $b = 77.2$ Å, $c = 84.3$ Å and contains one CaMKKβ·STO-609 complex in the asymmetric unit. The crystal structure of the CaMKKβ·STO-609 complex was determined by the molecular replacement method and refined to 2.4 Å resolution (Table 1). The final model includes residues 160–173, 176–199, and 231–448 of CaMKKβ, one STO-609 molecule, and 53 water molecules. A conserved Gly-rich segment (^{172}GKGSYG^{177}) in the phosphate-binding loop (P-loop) was partially disordered in the crystal structure. In addition, the characteristic Arg-Pro-rich insert (RP-insert) of the two CaMKK isoforms (Fig. 1*B*) was not identified due to lack of electron density, indicating a high degree of mobility in this region.

Fig. 2*A* shows a ribbon representation of the crystal structure of the CaMKKβ·STO-609 complex. STO-609 is bound in the ATP-binding pocket of the CaMKKβ KD, which is consistent with the previous report that the inhibition mechanism of STO-609 is ATP-competitive (25). The CaMKKβ KD adopts the canonical protein kinase fold, except that there is no counterpart to the αD helix. The equivalent region of CaMKKβ contains the conserved Pro residues among the CaMKKs (Fig. 1*B*) and forms a loop (the β5-αE loop) rather than a helical turn. The region surrounding the β5-αE loop displays a hydrophobic molecular surface (Fig. 2*B*), which may be involved in the binding of the substrate sequence (see next section for details).

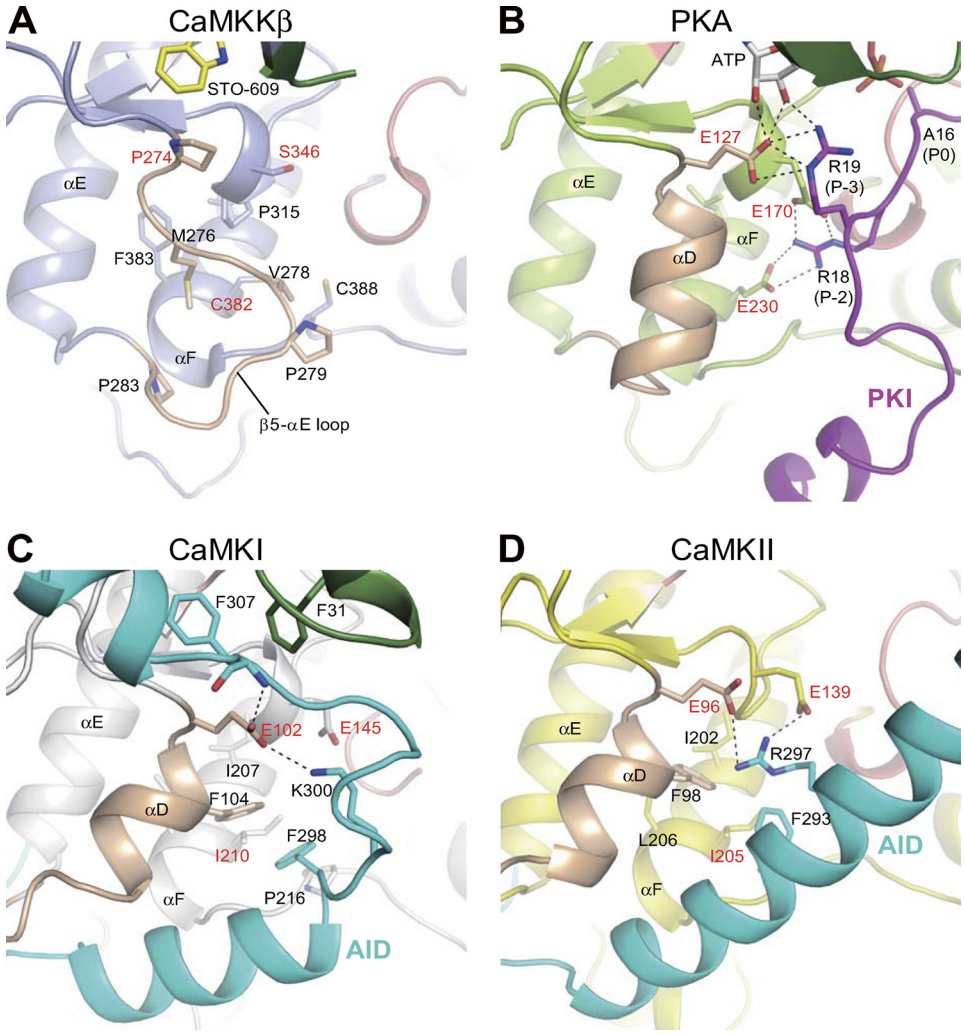

FIGURE 3. **Close-up views of the region surrounding the β5-αE loop of CaMKKβ (*A*) in comparison with the equivalent region of the PKA-PKI complex (*B*), CaMKI (*C*), and CaMKII (*D*).** The coloring of the elements is the same as in Fig. 2. Hydrogen bonds are indicated as *dashed lines*.

A structural comparison with other protein kinases revealed that the CaMKKβ·STO-609 complex adopts a closed conformation (36), resembling the active state of kinases such as PKA (PDB code 1ATP) (37) (Fig. 2*C*, *left panel*) (root mean square deviation 1.6 Å over 245 Cα atoms, 73% of the total 336 Cα atoms) and phosphorylase kinase (PDB code 1PHK) (38) (root mean square deviation 1.7 Å over 252 Cα atoms, 91% of the total 277 Cα atoms), with sequence identities of 36 and 31%, respectively. The CaMKKβ structure in this study is quite different from the previous structures of CaMKI (PDB code 1A06) (17) and CaMKII (PDB code 2BDW) (39) (Fig. 2*C*, *middle* and *right panels*), which adopt an open conformation with the N-lobe located away from the C-lobe due to the presence of the AID in the C terminus.

Substrate Sequence-binding region of CaMKKβ—CaMKK lacks the conserved acidic residues that, in many other kinases, recognize basic residues in substrates. To identify the substrate specificity determinants of CaMKK, we compared the structure of CaMKKβ with that of PKA complexed with a pseudosubstrate, PKA inhibitor (PKI). Glu^{127} of PKA interacts with the Arg residue at the P-3 position of PKI, but in CaMKKβ, this acidic residue is replaced by Pro (Pro^{274}) (Fig. 3, *A* and *B*). In addition, Glu^{170} and Glu^{230} of PKA, which interact with the Arg residue at the P-2 position of PKI, are replaced with Ser^{316} and Cys^{382}, respectively, in CaMKKβ. These CaMKKβ residues are clustered with the conserved hydrophobic residues among the CaMKKs, creating a hydrophobic pocket that is suitable for the accommodation of hydrophobic residues in substrates (Fig. 3*A*). Consistent with these observations, an inspection of the sequences around the phosphorylation sites of various CaMKK substrates, CaMKI (^{172}GSVLSTA^{178}), CaMKIV (^{191}QVLMKTV^{197}), PKB (^{303}GATMKTF^{309}), AMPK (^{167}GEFLRTS^{173}), and SAD-B (^{184}DSLLETS^{190}), suggested that CaMKK prefers hydrophobic or non-polar residues, rather than basic residues, at the P-3 and P-2 positions of the substrate.

The current structure of the CaMKKβ KD revealed that CaMKKβ lacks the αD helix that, in CaMKI and CaMKII, is involved in hydrophobic interactions with the AID (Fig. 3, *A*, *C*, and *D*). In addition, the basic residues of the CaMKI and CaMKII AIDs form hydrogen bonds with the conserved Glu residues (Glu^{102} and Glu^{96} of the CaMKI and CaMKII KDs, respectively), whereas CaMKKβ lacks the corresponding residue and instead has Pro^{274}. Therefore, the interactive structure between the KD and AID of CaMKKβ should be quite different

from those of CaMKI and CaMKII. Indeed, the length, the sequence, and the structure in the CaM-bound form (18–20) of the AID of CaMKK all differ from those of the AID of CaMK.

CaMKKβ Is an Intrinsically Active Kinase Lacking the Activation Loop Phosphorylation Site—In many protein kinases, phosphorylation of the activation loop site(s) is required for the folding of the activation segment into the active-state conformation, which promotes substrate binding and catalysis (40, 41). CaMKK possesses Ser and Thr residues, which are candidates for the phosphorylation sites, within the activation loop. However, the current structure of the CaMKKβ·STO-609 complex revealed that although the activation loop Ser and Thr residues of CaMKKβ were not phosphorylated, the activation segment was folded in the active, "DFG-in" conformation. The conserved Phe residue (Phe^{331}) within the DFG motif interacts with the αC helix, stabilizing a catalytically necessary ion pair (Glu^{236} and Lys^{194}) (Fig. 4*A*). This result clearly indicates that CaMKKβ does not require activation loop phosphorylation to adopt the active conformation. Intriguingly, Asn^{346} of CaMKKβ, rather than the adjacent Ser and Thr residues (Ser^{345} and Thr^{347}), is spatially equivalent to the phosphorylated Thr residue (Thr^{197}) of PKA, in which the phosphate group of the phosphothreonine forms hydrogen bonds with the catalytic loop (Arg^{165}) and the activation loop (Lys^{189}) residues (Fig. 4, *A* and *B*).

The activation loop of CaMKKβ is stabilized by a number of intramolecular interactions (Fig. 4*A*). The main-chain carbonyl and imino groups of Leu^{309}, respectively, hydrogen-bond with the main-chain imino and carbonyl groups of Asn^{335} and form a short anti-parallel β sheet between β6 and β9. Similarly, the main-chain carbonyl and imino groups of Leu^{344}, respectively, hydrogen-bond with the main-chain imino and carbonyl groups of Phe^{366}, thus forming another short anti-parallel β sheet between β10 and β11. In addition, the side chain of Asn^{335} hydrogen-bonds with the catalytic loop Arg residue (Arg^{311}), which forms hydrogen bonds with the main-chain and the side-chain carbonyl groups of Asn^{346}. On the other hand, the side chains of Phe^{337}, Ala^{342}, and Leu^{344} form hydrophobic interactions with those of Leu^{309} and Arg^{311}. Furthermore, the side chain of Thr^{347} hydrogen-bonds with the main-chain carbonyl group of Ser^{360} from αEF. All of these residues are highly conserved in the CaMKKβ proteins among various species. The activation loop of CaMKKβ has some interactions with the symmetry-related molecule, but the buried surface is relatively small (~530 Å^2, corresponding to 4.1% of the total surface area), and the interacting residues are not well conserved.

CaMKII, like CaMKKβ, lacks a phosphorylation site in the activation loop. A comparison of the activation loop of CaMKKβ to that of CaMKII (Fig. 4, *A* and *C*) revealed a structural similarity in that the conserved catalytic loop Arg residue (Arg^{311} in CaMKKβ and Arg^{134} in CaMKII) hydrogen-bonds directly with the main-chain carbonyl group of the activation loop residue (Asn^{346} in CaMKKβ and His^{171} in CaMKII). Another common feature is the existence of hydrophobic interactions between the side chains of the activation loop residues, although the participating residues are not conserved between CaMKKβ and CaMKII (Phe^{337}, Ala^{342}, and Leu^{344} in CaMKKβ and Ile^{161}, Val^{163}, and His^{171} in CaMKII).

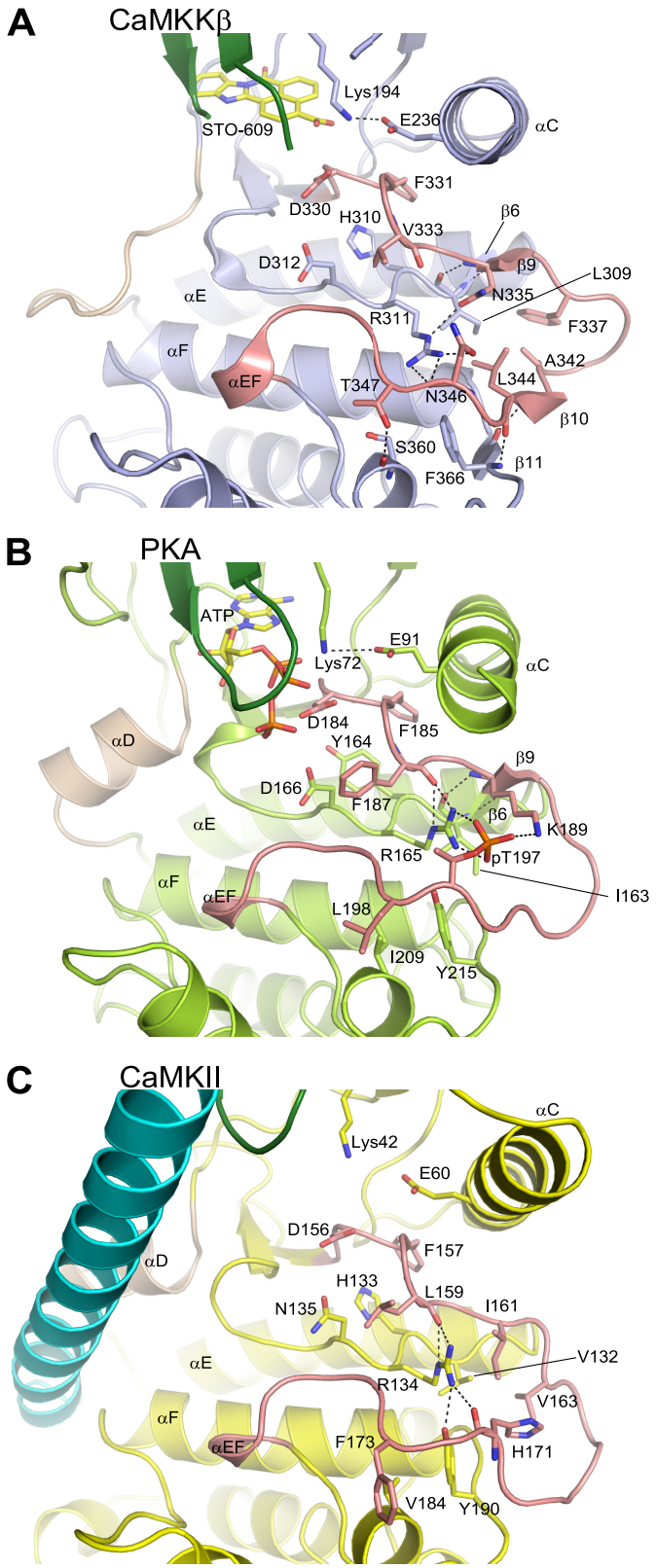

FIGURE 4. **Comparison of the activation segments of CaMKKβ (*A*), PKA (*B*), and CaMKII (*C*), showing the stabilization of the activation loop conformation.** The activation segment is colored *salmon*. Hydrogen bonds are indicated as *dashed lines*.

In CaMKKα, the residue corresponding to Asn^{346} of CaMKKβ, which is located in the equivalent position of the phosphorylated Ser/Thr residue within the activation loop, is

Ser[309], which is a good candidate for the regulatory phosphorylation site. However, except for Asn[346], all of the CaMKKβ residues that stabilize the activation loop are conserved in CaMKKα. Thus, it is possible that CaMKKα may also adopt an active-state conformation without phosphorylation of the activation loop Ser residue (Ser[309]).

Characterization of the Kinase Activity—We next examined whether human CaMKKβ KD, displaying a constitutively active kinase structure, is indeed an active kinase. For this purpose, we used the human CaMKKβ KD protein purified for crystallization and a synthetic substrate peptide containing the sequence around the phosphorylation site of AMPK ([167]GEFLRTSCGSP[177]). When the purified CaMKKβ KD protein was incubated with ATP under phosphorylation conditions, significant ATP consumption was observed only in the presence of the AMPK peptide, indicating that the CaMKKβ KD has an activity to phosphorylate the AMPK peptide. The phosphorylation activity of the purified CaMKKβ KD (7.52 nmol min^{-1} $nmol^{-1}$) was much higher than that of the full-length CaMKKβ (1.22 nmol min^{-1} $nmol^{-1}$) (Table 2). In addition, we confirmed that the STO-609-mediated inhibition of the CaMKKβ KD was similar to that of the full-length CaMKKβ (Table 2). The result clearly indicates that the CaMKKβ KD is intrinsically active without phosphorylation of the activation loop. Considering its function at the top of the CaMK cascade, it is reasonable that CaMKK is an intrinsically active kinase that can be activated only by Ca^{2+}/CaM.

TABLE 2
Inhibition of CaMKKβ by STO-609

	Phosphorylation activity (nmol/min/nmol CaMKKβ)		
STO-609	0 μM	0.5 μM	% of inhibition
CaMKKβ KD	7.52 ± 0.48	2.96 ± 0.40	60.7 ± 2.8
CaMKKβ	1.22 ± 0.17	0.502 ± 0.001	58.5 ± 5.7

Selective Interactions of CaMKKβ with STO-609—The planar molecule STO-609 is bound to the CaMKKβ KD, and its carboxylic acid moiety is slightly tilted (Fig. 5*A*). This conformation enables the inhibitor to fit within a narrow pocket of the CaMKKβ KD that adopts a closed conformation (Fig. 5*B*). The interactions between STO-609 and CaMKKβ are mostly hydrophobic, involving Ile[171], Val[179], Ala[192], Val[249], and Phe[267] from the N-lobe and Gly[273], Pro[274], Leu[319], and Asp[330] from the C-lobe (Fig. 5*A*). In addition, STO-609 hydrogen-bonds with the backbones of Val[270] and Asp[330], as well as with the conserved catalytic residue Glu[236], in a water-mediated manner. CaMKKβ is reportedly more sensitive to STO-609 than CaMKKα (25). As shown in Fig. 5*C*, among the CaMKKβ residues that interact with STO-609, only Val[270] is replaced, by Leu, in CaMKKα. This result suggests that the Val to Leu replacement at this position causes the different STO-609 sensitivities between the CaMKK isoforms. Consistently, mutations of the corresponding Val residue of rat CaMKKβ (Val[269]) to residues with bulky side chains, including Leu, His, Met, and Phe, significantly decreased the sensitivity to STO-609 (42). Based on the structure, we suggest that this is due to steric inhibition of STO-609 binding.

We next compared the amino acid sequence of the STO-609-binding site of CaMKKβ with those of other protein kinases, such as CaMKI, CaMKII, CaMKIV, PKA, AMPK, and LKB1, which are much less sensitive to STO-609 than CaMKKα and

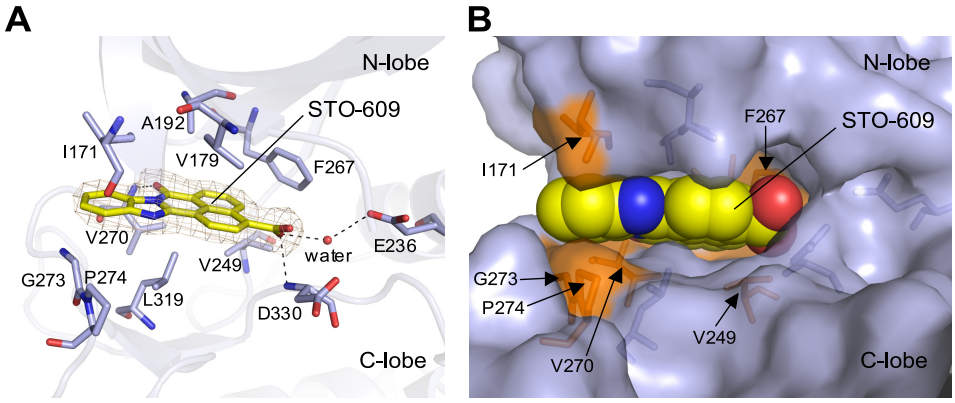

C

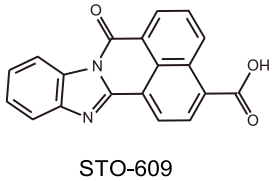

STO-609

	STO-609-binding residues										
	171	179	192	236	249	267	270	273	274	319	330
CaMKK β	I	V	A	E	V	F	V	G	P	L	D
CaMKK α	I	V	A	E	V	F	L	G	P	L	D
CaMKII	I	V	A	E	V	F	V	G	E	L	D
CaMKI	L	V	A	E	V	M	V	G	E	L	D
PKA	L	V	A	E	V	M	V	G	E	L	D
CaMKIV	L	V	A	E	I	L	V	G	E	L	D
AMPK	L	V	A	E	I	M	V	G	E	L	D
LKB1	L	V	A	E	I	M	V	Q	E	L	D

FIGURE 5. **The STO-609-binding site.** *A*, the binding site structure with the STO-609 modeled in the $2F_o - F_c$ electron density map. The STO-609 and the residues of CaMKKβ that coordinate STO-609 are represented as *stick models*. Hydrogen bonds are indicated as *dashed lines*. *B*, the inhibitor-binding residues, shown with a superposition of their molecular surfaces. The STO-609 is shown in a *sphere representation*. *C*, chemical diagram of STO-609 and sequence comparison of the STO-609-binding residues of CaMKKβ with other protein kinases.

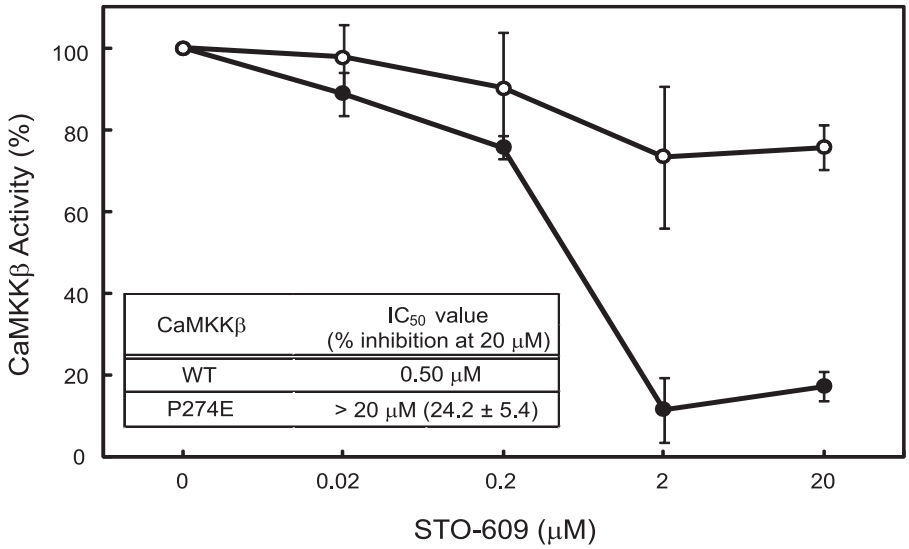

FIGURE 6. **Effect of STO-609 on the activities of the wild-type and P274E mutant CaMKK*β* KDs.** The wild-type (WT) (*closed circles*) and P274E mutant (*open circles*) CaMKK*β* KDs were assayed to measure the inhibitory effects of STO-609 (at the indicated concentrations) on their activities to phosphorylate the AMPK peptide. The experiments were performed in duplicate for each condition, as described under "Experimental Procedures." The amounts of ATP consumption in the absence of STO-609 were set to 100. *Error bars* indicate S.D.

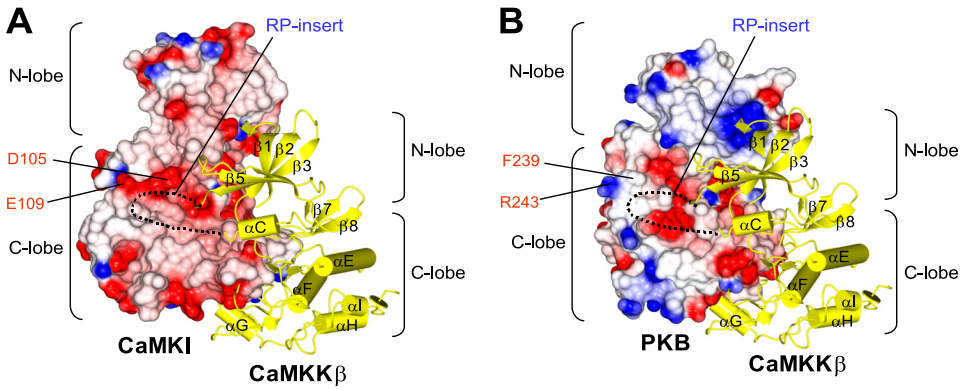

FIGURE 7. **Hypothetical models of the heterodimeric CaMKK*β*·CaMKI (*A*) and CaMKK*β*·PKB (*B*) complexes.** The CaMKK*β* KD (*yellow ribbons*) is docked onto the electrostatic surfaces of the CaMKI KD and the PKB KD (*red*, negative charge; *blue*, positive charge). The disordered RP-insert region of the CaMKK*β* KD is indicated as *dashed lines*. Selected residues in the CaMKI KD and the PKB KD are indicated.

CaMKK*β*. The inhibitor potencies of STO-609 against these protein kinases are different, and the IC_{50} values were previously ranked as CaMKK*β* < CaMKK*α* < CaMKII < CaMKI = PKA < CaMKIV (25) and as CaMKK*β* < AMPK < LKB1 (43). As shown in Fig. 5*C*, the CaMKK*β* residues that interact with STO-609, such as Ile^{171}, Val^{249}, Phe^{267}, Gly^{273}, and Pro^{274}, are replaced with various residues in these protein kinases, and the degrees of the amino acid replacements correlate well with the different inhibitor potencies displayed by STO-609. In particular, Pro^{274} of CaMKK*β* is replaced by Glu in all of these protein kinases except for CaMKK*α*, suggesting that Pro at this position is the most important determinant for the selective binding of STO-609 in CaMKK as compared with the other protein kinases.

This finding led us to examine the effect of the CaMKK*β* P274E mutation on the inhibition by STO-609. As shown in Fig. 6, the P274E mutation significantly reduced the inhibitory effect of STO-609 on the CaMKK*β* KD. Although the kinase activity of the wild-type CaMKK*β* KD was almost completely inhibited in the presence of 20 μM STO-609, the P274E mutant was only slightly affected (24.2% inhibition) by the same concentration of STO-609. The IC_{50} value of STO-609 for the P274E mutant was estimated to be more than 20 μM, which was much higher than that of the wild-type protein (IC_{50} = 0.50 μM). This mutagenesis result indicated that the Pro side chain at this position contributes to the selective inhibition of CaMKK*β* by STO-609.

In the current structure of the CaMKK*β*·STO-609 complex, Pro^{274} is located at the gate of the STO-609-binding pocket, and the pyrrolidine ring forms hydrophobic contacts with the inhibitor (Fig. 5*B*). It is therefore likely that the presence of an acidic residue, which in the other protein kinases recognizes a basic residue at the P-3 position of the substrate (Fig. 3, *B–D*), in place of the Pro in CaMKK*α* and CaMKK*β*, would reduce the binding of STO-609 due to the loss of hydrophobic contacts.

Implications for Selective Substrate Protein Recognition by the RP-insert—It was previously demonstrated that PKB is a relatively poor substrate for CaMKK as compared with the downstream kinases (CaMKI and CaMKIV) (44). In addition, the intact CaMKI and CaMKIV proteins are much better substrates for CaMKK as compared with synthetic peptides containing the sequence around the phosphorylation sites of CaMKI and

CaMKIV (45). The RP-insert of CaMKK is required for the selective high affinity interactions with CaMKI and CaMKIV, although it is dispensable for its autophosphorylation, CaMKIV peptide phosphorylation, and PKB activation (46). Because the Arg to Glu mutations within the RP-insert of rat CaMKKα drastically reduced its ability to activate CaMKIV (46), it is likely that the positively charged Arg residues within the CaMKK RP-insert are required for the recognition of the negatively charged residues in CaMKI and CaMKIV.

To gain insight of how CaMKKβ recognizes its substrate kinases, we generated docking models for the CaMKKβ·CaMKI and CaMKKβ·PKB complexes (Fig. 7) by superposing the crystal structures of CaMKKβ (this study), CaMKI (PDB code 1A06) (17), and PKB (PDB code 1GZN) (47) onto the structure of p38 MAPK·MAPK-activated kinase 2 complex (PDB code 2OZA) (48). These structural models suggested that the negatively charged residues in the αD helix of CaMKI (Asp^{105} and Glu^{109} in rat sequence), which are conserved in CaMKIV but not in PKB (Phe^{239} and Arg^{243}), may interact with the RP-insert of CaMKKβ. Intriguingly, the mutation of the corresponding Asp residue (Asp^{108}) to Arg in the human CaMKI KD reduced its ability to be phosphorylated by the CaMKKβ KD (supplemental Fig. 1). Therefore, it is possible that the Asp residue in the αD helix of CaMKI may be involved in the interaction with CaMKKβ. Although the residues of CaMKKβ that interact with this Asp residue of CaMKI have not been identified, based on the sequence conservation between CaMKKs (46), it is conceivable that the Arg residues within the RP-insert are involved in this interaction. The determination of the structure of the CaMKKβ·CaMKI complex will clarify the specific features of binding between these proteins.

In conclusion, this study has demonstrated the unique structural properties of the CaMKKβ KD, which provide a molecular basis for understanding the known biochemical properties of CaMKKβ and the distinct STO-609 sensitivity between the CaMKKα and CaMKKβ isoforms. Our structure of the CaMKKβ·STO-609 complex also provides a structural basis for designing novel inhibitors to specifically block CaMKKβ and related protein kinases.

Acknowledgments—We thank Hideaki Niwa, Takashi Umehara, Mitsutoshi Toyama, Mio Inoue, Mari Aoki, Mio Goto, Ken Ishii, Naomi Ohbayashi, Tomomi Uchikubo-Kamo, Ryogo Akasaka, and Kazushige Katsura for technical assistance. We are grateful to Dr. Osamu Ohara (Kazusa DNA Research Institute, Japan) for the CaMKKβ clone (KIAA0787). We thank the members of the Support Unit for Bio-material Analysis, RIKEN BSI Research Resource Center, and especially Reiko Ito, Junko Ishikawa, and Aya Abe, for AMPK peptide synthesis.

REFERENCES

1. Soderling, T. R. (1999) *Trends Biochem. Sci.* **24,** 232–236
2. Soderling, T. R., and Stull, J. T. (2001) *Chem. Rev.* **101,** 2341–2352
3. Corcoran, E. E., and Means, A. R. (2001) *J. Biol. Chem.* **276,** 2975–2978
4. Wayman, G. A., Lee, Y. S., Tokumitsu, H., Silva, A. J., and Soderling, T. R. (2008) *Neuron* **59,** 914–931
5. Haribabu, B., Hook, S. S., Selbert, M. A., Goldstein, E. G., Tomhave, E. D., Edelman, A. M., Snyderman, R., and Means, A. R. (1995) *EMBO J.* **14,** 3679–3686
6. Selbert, M. A., Anderson, K. A., Huang, Q. H., Goldstein, E. G., Means, A. R., and Edelman, A. M. (1995) *J. Biol. Chem.* **270,** 17616–17621
7. Tokumitsu, H., Enslen, H., and Soderling, T. R. (1995) *J. Biol. Chem.* **270,** 19320–19324
8. Kitani, T., Okuno, S., and Fujisawa, H. (1997) *J. Biochem.* **122,** 243–250
9. Anderson, K. A., Means, R. L., Huang, Q. H., Kemp, B. E., Goldstein, E. G., Selbert, M. A., Edelman, A. M., Fremeau, R. T., and Means, A. R. (1998) *J. Biol. Chem.* **273,** 31880–31889
10. Enslen, H., Tokumitsu, H., Stork, P. J., Davis, R. J., and Soderling, T. R. (1996) *Proc. Natl. Acad. Sci. U.S.A.* **93,** 10803–10808
11. Schmitt, J. M., Wayman, G. A., Nozaki, N., and Soderling, T. R. (2004) *J. Biol. Chem.* **279,** 24064–24072
12. Wayman, G. A., Tokumitsu, H., and Soderling, T. R. (1997) *J. Biol. Chem.* **272,** 16073–16076
13. Yano, S., Tokumitsu, H., and Soderling, T. R. (1998) *Nature* **396,** 584–587
14. Witczak, C. A., Sharoff, C. G., and Goodyear, L. J. (2008) *Cell. Mol. Life Sci.* **65,** 3737–3755
15. Fujimoto, T., Yurimoto, S., Hatano, N., Nozaki, N., Sueyoshi, N., Kameshita, I., Mizutani, A., Mikoshiba, K., Kobayashi, R., and Tokumitsu, H. (2008) *Biochemistry* **47,** 4151–4159
16. Tokumitsu, H., Wayman, G. A., Muramatsu, M., and Soderling, T. R. (1997) *Biochemistry* **36,** 12823–12827
17. Goldberg, J., Nairn, A. C., and Kuriyan, J. (1996) *Cell* **84,** 875–887
18. Osawa, M., Tokumitsu, H., Swindells, M. B., Kurihara, H., Orita, M., Shibanuma, T., Furuya, T., and Ikura, M. (1999) *Nat. Struct. Biol.* **6,** 819–824
19. Kurokawa, H., Osawa, M., Kurihara, H., Katayama, N., Tokumitsu, H., Swindells, M. B., Kainosho, M., and Ikura, M. (2001) *J. Mol. Biol.* **312,** 59–68
20. Clapperton, J. A., Martin, S. R., Smerdon, S. J., Gamblin, S. J., and Bayley, P. M. (2002) *Biochemistry* **41,** 14669–14679
21. Tokumitsu, H., and Soderling, T. R. (1996) *J. Biol. Chem.* **271,** 5617–5622
22. Tokumitsu, H., Muramatsu, M., Ikura, M., and Kobayashi, R. (2000) *J. Biol. Chem.* **275,** 20090–20095
23. Tokumitsu, H., Iwabu, M., Ishikawa, Y., and Kobayashi, R. (2001) *Biochemistry* **40,** 13925–13932
24. Davare, M. A., Saneyoshi, T., Guire, E. S., Nygaard, S. C., and Soderling, T. R. (2004) *J. Biol. Chem.* **279,** 52191–52199
25. Tokumitsu, H., Inuzuka, H., Ishikawa, Y., Ikeda, M., Saji, I., and Kobayashi, R. (2002) *J. Biol. Chem.* **277,** 15813–15818
26. Kigawa, T., Yabuki, T., Matsuda, N., Matsuda, T., Nakajima, R., Tanaka, A., and Yokoyama, S. (2004) *J. Struct. Funct. Genomics* **5,** 63–68
27. Kigawa, T., Matsuda, T., Yabuki, T., and Yokoyama, S. (2007) *Cell-free Protein Synthesis* (Spirin A. S., and Swartz, J. R., eds) pp. 83–97, Wiley-VCH, Weinheim, Germany
28. Otwinowski, Z., and Minor, W. (1997) *Methods Enzymol.* **276,** 307–326
29. Read, R. J. (2001) *Acta Crystallogr. D Biol. Crystallogr.* **57,** 1373–1382
30. Collaborative Computational Project, Number 4 (1994) *Acta Crystallogr. D Biol. Crystallogr.* **50,** 760–763
31. Emsley, P., and Cowtan, K. (2004) *Acta Crystallogr. D Biol. Crystallogr.* **60,** 2126–2132
32. Brünger, A. T., Adams, P. D., Clore, G. M., DeLano, W. L., Gros, P., Grosse-Kunstleve, R. W., Jiang, J. S., Kuszewski, J., Nilges, M., Pannu, N. S., Read, R. J., Rice, L. M., Simonson, T., and Warren, G. L. (1998) *Acta Crystallogr. D Biol. Crystallogr.* **54,** 905–921
33. Laskowski, R. A., MacArthur, M. W., Moss, D. S., and Thornton, J. M. (1993) *J. Appl. Crystallogr.* **26,** 283–291
34. Holm, L., and Sander, C. (1993) *J. Mol. Biol.* **233,** 123–138
35. DeLano, W. L. (2010) *The PyMOL Molecular Graphics System*, version 1.3r1, Schrödinger, LLC, New York
36. Cox, S., Radzio-Andzelm, E., and Taylor, S. S. (1994) *Curr. Opin. Struct. Biol.* **4,** 893–901
37. Zheng, J., Trafny, E. A., Knighton, D. R., Xuong, N. H., Taylor, S. S., Ten Eyck, L. F., and Sowadski, J. M. (1993) *Acta Crystallogr. D Biol. Crystallogr.* **49,** 362–365
38. Owen, D. J., Noble, M. E., Garman, E. F., Papageorgiou, A. C., and Johnson, L. N. (1995) *Structure* **3,** 467–482
39. Rosenberg, O. S., Deindl, S., Sung, R. J., Nairn, A. C., and Kuriyan, J. (2005)

Cell **123,** 849–860
40. Johnson, L. N., Noble, M. E., and Owen, D. J. (1996) *Cell* **85,** 149–158
41. Nolen, B., Taylor, S., and Ghosh, G. (2004) *Mol. Cell* **15,** 661–675
42. Tokumitsu, H., Inuzuka, H., Ishikawa, Y., and Kobayashi, R. (2003) *J. Biol. Chem.* **278,** 10908–10913
43. Hawley, S. A., Pan, D. A., Mustard, K. J., Ross, L., Bain, J., Edelman, A. M., Frenguelli, B. G., and Hardie, D. G. (2005) *Cell Metabolism* **2,** 9–19
44. Okuno, S., Kitani, T., Matsuzaki, H., Konishi, H., Kikkawa, U., and Fujisawa, H. (2000) *J. Biochem.* **127,** 965–970
45. Kitani, T., Ishida, A., Okuno, S., Takeuchi, M., Kameshita, I., and Fujisawa, H. (1999) *J. Biochem.* **125,** 1022–1028
46. Tokumitsu, H., Takahashi, N., Eto, K., Yano, S., Soderling, T. R., and Muramatsu, M. (1999) *J. Biol. Chem.* **274,** 15803–15810
47. Yang, J., Cron, P., Thompson, V., Good, V. M., Hess, D., Hemmings, B. A., and Barford, D. (2002) *Mol. Cell* **9,** 1227–1240
48. White, A., Pargellis, C. A., Studts, J. M., Werneburg, B. G., and Farmer, B. T., 2nd (2007) *Proc. Natl. Acad. Sci. U.S.A.* **104,** 6353–6358
49. Gouet, P., Courcelle, E., Stuart, D. I., and Métoz, F. (1999) *Bioinformatics* **15,** 305–308
50. Potterton, L., McNicholas, S., Krissinel, E., Gruber, J., Cowtan, K., Emsley, P., Murshudov, G. N., Cohen, S., Perrakis, A., and Noble, M. (2004) *Acta Crystallogr. D* **60,** 2288–2294